Exp. Anim. 62(4), 333–346, 2013

—Original—

Compound Heterozygosity of the Functionally Null *Cdh23$^{v\text{-}ngt}$* and Hypomorphic *Cdh23^{ahl}* Alleles Leads to Early-onset Progressive Hearing Loss in Mice

Yuki MIYASAKA[1,2], Sari SUZUKI[1,3], Yasuhiro OHSHIBA[1,2], Kei WATANABE[1,4], Yoshihiko SAGARA[3]*, Shumpei P. YASUDA[1], Kunie MATSUOKA[1], Hiroshi SHITARA[5], Hiromichi YONEKAWA[5], Ryo KOMINAMI[2], and Yoshiaki KIKKAWA[1]

[1]*Mammalian Genetics Project, Tokyo Metropolitan Institute of Medical Science, 2–1–6 Kamikitazawa, Setagaya-ku, Tokyo 156-8506, Japan*
[2]*Graduate School of Medical and Dental Sciences, Niigata University, 1–757 Asahimachi, Niigata 951-8510, Japan*
[3]*Department of Bioproduction, Tokyo University of Agriculture, 196 Yasaka, Abashiri, Hokkaido 099-2493, Japan*
[4]*Graduate School of Life and Environmental Sciences, University of Tsukuba, 1–1–1 Tennodai, Tsukuba, Ibaraki 305-8577, Japan*
[5]*Center for Basic Technology Research, Tokyo Metropolitan Institute of Medical Science, 2–1–6 Kamikitazawa, Setagaya-ku, Tokyo 156-8506, Japan*

Abstract: The waltzer (*v*) mouse mutant harbors a mutation in Cadherin 23 (*Cdh23*) and is a model for Usher syndrome type 1D, which is characterized by congenital deafness, vestibular dysfunction, and prepubertal onset of progressive retinitis pigmentosa. In mice, functionally null *Cdh23* mutations affect stereociliary morphogenesis and the polarity of both cochlear and vestibular hair cells. In contrast, the murine *Cdh23^{ahl}* allele, which harbors a hypomorphic mutation, causes an increase in susceptibility to age-related hearing loss in many inbred strains. We produced congenic mice by crossing mice carrying the *v niigata* (*Cdh23$^{v\text{-}ngt}$*) null allele with mice carrying the hypomorphic *Cdh23^{ahl}* allele on the C57BL/6J background, and we then analyzed the animals' balance and hearing phenotypes. Although the *Cdh23$^{v\text{-}ngt/ahl}$* compound heterozygous mice exhibited normal vestibular function, their hearing ability was abnormal: the mice exhibited higher thresholds of auditory brainstem response (ABR) and rapid age-dependent elevation of ABR thresholds compared with *Cdh23$^{ahl/ahl}$* homozygous mice. We found that the stereocilia developed normally but were progressively disrupted in *Cdh23$^{v\text{-}ngt/ahl}$* mice. In hair cells, CDH23 localizes to the tip links of stereocilia, which are thought to gate the mechanoelectrical transduction channels in hair cells. We hypothesize that the reduction of *Cdh23* gene dosage in *Cdh23$^{v\text{-}ngt/ahl}$* mice leads to the degeneration of stereocilia, which consequently reduces tip link tension. These findings indicate that CDH23 plays an important role in the maintenance of tip links during the aging process.

Key words: age-related hearing loss, cadherin 23, hair cell, mouse mutant, stereocilia

(Received 29 April 2013 / Accepted 14 May 2013)

Address corresponding: Y. Kikkawa, Mammalian Genetics Project, Department of Genome Medicine, Tokyo Metropolitan Institute of Medical Science, 2–1–6 Kamikitazawa, Setagaya-ku, Tokyo 156-8506, Japan

**Current address: Technology and Development Team for Mouse Phenotype Analysis, RIKEN BioResource Center, 3–1–1 Koyadai, Tsukuba, Ibaraki 305-0074, Japan*

Introduction

Inbred mouse strains allow many models for investigating human diseases. More than 450 inbred strains have been established, providing different genotypes and phenotypes for genetic and other studies [3, 35]. For studies of human genetic deafness, inbred mouse strains are excellent animal models because the mouse auditory system is anatomically similar to that of humans [2, 33]. As found in humans, inbred strains also differ in their predisposition to age-related hearing loss (AHL) [15, 25]. One AHL susceptibility gene, *ahl*, is located on chromosome 10 [12], and *ahl* possesses a functional SNP (G753A) in the coding sequence of cadherin 23 (*Cdh23*) that creates a splice junction leading to the expression of a transcript lacking exon 7 [26]. CDH23 is a Ca^{2+}-mediated single transmembrane cell-cell adhesion molecule containing 27 extracellular cadherin repeats (ECs) followed by a single transmembrane domain and a short intracellular domain [7, 23, 27]. The susceptible allele is shared by approximately 80% of inbred strains with AHL such as the C57BL/6J strain [26]. The C57BL/6J strain with homozygosity of the $Cdh23^{ahl}$ allele expresses only exon 7-lacking CDH23 and exhibits late-onset AHL, i.e., severe hearing loss at 9–12 months of age [9, 15, 21, 36]. Conversely, inbred strains transmitting the $Cdh23^{753G}$ resistant allele mostly maintain life-long hearing, as exemplified in C3H/HeN mice [15].

By contrast, functionally null waltzer ($Cdh23^{v}$) mutations of *Cdh23* in mice lead to the shaker/waltzer phenotype, which is characterized by hearing loss and vestibular dysfunction. Several functionally null mutations of *Cdh23* have been reported, including $Cdh23^{v}$ and waltzer niigata ($Cdh23^{v\text{-}ngt}$), and homozygous $Cdh23^{v}$ mice exhibit the typical circling, head-tossing, hyperactive behavior, and congenital profound hearing loss caused by the degeneration of stereocilia on hair cells of the inner ear [7, 34, 37]. In the stereocilia, CDH23 expression is restricted to the links that connect a stereocilium to the side of a neighboring stereocilium, including the tip links of mature mice and the transient links that form at fetal stages [13, 16, 17, 20, 29, 30]. $Cdh23^{v}$ mice exhibit an irregular bundle morphology, poor maintenance and loss of the normal stereocilia pattern [7, 17, 34], as well as stereocilia that are splayed and of irregular length, suggesting that loss of CDH23 in $Cdh23^{v}$ mice leads to reduced tension between stereocilia and subsequent stereocilia degeneration [17].

Cdh23 is thus an important gene that underlies not only AHL but also stereociliary development in mice. However, the relationship between CDH23 on the tip links in stereocilia and hearing impairment in aged mice remains obscure. Accordingly, we generated compound heterozygous mice of the C57BL/6J background with one null allele of $Cdh23^{v\text{-}ngt}$ and one hypomorphic allele of $Cdh23^{ahl}$ and examined hearing loss and hair cells in mice of different ages. Our results indicate that these $Cdh23^{v\text{-}ngt/ahl}$ compound heterozygotes show early-onset progressive hearing loss relative to $Cdh23^{ahl/ahl}$ mice and that this hearing loss is associated with progressive degeneration of stereocilia, suggesting that CDH23 plays an important role in the maintenance of tip links during the aging process. This study also provides an evaluation of their potential as a new model of hearing impairment caused by the *Cdh23* mutation.

Materials and Methods

Mice

ICR-$Cdh23^{v\text{-}ngt/v\text{-}ngt}$ homozygous mutants were obtained from Niigata University (Niigata, Japan) and were then crossed with C57BL/6J mice (Clea Japan, Tokyo, Japan) that had a $Cdh23^{ahl}$ allele [15, 26]. The F_1 $Cdh23^{v\text{-}ngt/ahl}$ compound heterozygous mice were backcrossed with C57BL/6J mice for 20 generations at the Tokyo Metropolitan Institute of Medical Science (Tokyo, Japan), and the $Cdh23^{v\text{-}ngt/ahl}$ compound heterozygote and $Cdh23^{v\text{-}ngt/v\text{-}ngt}$ homozygote offspring of breeder pairs consisting of a $Cdh23^{v\text{-}ngt/ahl}$ female and a $Cdh23^{v\text{-}ngt/v\text{-}ngt}$ male were used for all of the experiments. All of the procedures involving animals met the guidelines for the Proper Conduct of Animal Experiments, as defined by the Science Council of Japan, and were approved by the Animal Care and Use Committee of the Tokyo Metropolitan Institute of Medical Science.

Genotyping

The $Cdh23^{v\text{-}ngt}$ mutation was genotyped by PCR-RFLP analysis of pinna or tail genomic DNA. Genomic DNAs were extracted using KAPA Express Extract (Kapa Biosystems, Woburn, MA, USA). PCR amplification was carried out using a KAPA2G Fast PCR Kit (Kapa Biosystems) and primer set A (Supplementary Table 1: refer to J-STAGE at https://www.jstage.jst.go.jp/browse/expanim) and consisted of 40 cycles at 95°C for 20 s, 60°C for 20 s and 72°C for 5 s; the products were digested

with *Bst*NI (New England BioLabs, Ipswich, MA, USA) at 65°C for 1 h and then subjected to 4% agarose gel electrophoresis. The *Cdh23*^{ahl} mutation was confirmed by DNA sequencing of the products amplified by primer set B (Supplementary Table 1) using a BigDye Terminator kit (Life Technologies, Grand Island, NY, USA) and an Applied Biosystems 3130xl Genetic Analyzer.

RT-PCR

Total RNA was isolated from the inner ear using TRIzol Reagent (Life Technologies) and a TRIzol Plus Purification Kit (Life Technologies) according to the manufacturer's protocol. The total RNAs were treated with DNase I (Life Technologies), and then, cDNA was generated with a SuperScript VILO cDNA Synthesis Kit (Life Technologies) using 200 ng total RNA. Semiquantitative RT-PCR was carried out using a KOD FX Neo (TOYOBO, Osaka, Japan) and primer sets C, D and E (Supplementary Table 1) at 94°C for 2 min followed by 35 cycles of 98°C for 10 s and 68°C for 30 s; the products were then subjected to 2% agarose gel electrophoresis. We used a cDNA prepared from the cochlea of 1-month-old C3H/HeN mice as a control, and cDNA integrity was confirmed using a *Gapdh* primer set (Supplementary Table 1). Quantitative RT-PCR (qRT-PCR) was performed using a QuantiTect SYBR Green PCR Kit (Qiagen, Valencia, CA) and two primer sets, D and E, according to the manufacturer's protocol, and the products were analyzed on a LightCycler 480 Instrument (Roche Diagnostics, Tokyo, Japan). Signals specific to *Cdh23* were normalized against *Gapdh* (Qiagen, Mm_Gapdh_3). Samples from three independent experiments were analyzed in triplicate reactions for each cDNA.

Immunohistochemistry

The inner ears were removed from the heads of the mice and were fixed as described by Ding *et al.* [6]. The cochlear and vestibular sensory epithelia were dissected from the inner ear and were permeabilized in 0.25% Triton X-100 in PBS for 15–30 min and then subjected to three 5 min washes in PBS. After they were washed in PBS, nonspecific binding sites were blocked with 0.5% Blocking Reagent (Roche Molecular Biochemicals, Indianapolis, IN, USA) for 1 h at RT. Samples were incubated with affinity-purified CDH23 rabbit polyclonal antibody (PB240) diluted 1:50 in Can Get Signal Immunostain Solution B (TOYOBO) overnight at 4°C. The PB240 antibody was generated against peptide ATRPAPPDRERQ corresponding to a peptide used. For the antigen, an antibody was generated by Kazmierczak *et al.* [13] and was provided by K. Kamiya (Juntendo University Faculty of Medicine, Tokyo, Japan). Subsequently, samples were washed three times for 5 min in PBS, and an Alexa Fluor 568-conjugated secondary antibody (Life Technologies) and an Alexa Fluor 488-conjugated phalloidin (Life Technologies) were diluted to 20 μg/ml and 4 units/ml, respectively, in Can Get Signal Immunostain Solution B for 1 h at RT. Finally, they were washed three times for 5 min in PBS and then mounted onto a slide glass using PermaFluor. Fluorescence images were obtained using a Zeiss LSM 510 confocal microscope and processed using the Adobe Photoshop software. For the immunofluorescence labelling and hair cell quantification experiments, we used three images from three section preparations. The fluorescence intensity of CDH23 was analyzed using the ImageJ software (http://rsb.info.nih.gov/ij) to analyze confocal images that were taken under identical conditions and adjusted using the intensity of phalloidin labelling as a control.

Open-field behavior tests

Circling and activity behavior were measured using a DVTrack Video Tracking System (Muromachi Kikai, Tokyo, Japan). To quantify these behaviors, mice were placed in a 50 cm × 40 cm × 50 cm (W × H × L) open field. The movements of mice were tracked for 30 min, and the data on rotations (times/120 sec), average moving speed (cm/sec), and total travelled distance (cm) were collected and analyzed using CompACT VAS software ver. 3.1 (Muromachi Kikai).

Measurements of auditory brain stem response

The hearing ability of the mice was measured via the auditory brain stem response (ABR). Mice were anesthetized with an intraperitoneal injection of pentobarbital (60–80 mg/kg). ABRs were measured with a tone pip stimulus (4, 8, 16 and 32 kHz), using TDT System III (TDT, Alachua, FL, USA) and BioSigRP software (TDT). Both the right and left ears of the mice were used for the ABR measurement. ABRs were recorded with stainless steel needle electrodes inserted subcutaneously into the vertex (active), one side of the retroauricular region (inactive), and the opposite thigh (ground). For each frequency, a stimulus sound pressure level in decibels (dB SPL) of a tone pip consisting of 0.1 ms slopes, stimuli with a duration of 1 ms, and a repeat

interval of 50 ms was delivered in a free field. A sound source (speaker) was inserted into the external acoustic meatus of both ears of each mouse. ABR thresholds were obtained for each stimulus by reducing the SPL first in 10 dB steps and then up and down in 5 dB steps to identify the lowest level at which an ABR pattern could be recognized. ABR thresholds obtained from each ear were collected as separated data.

SEM

Mice were perfused through the heart with a buffer containing 2.5% glutaraldehyde and 0.1 M phosphate buffer (pH 7.4). Immediately after perfusion, the inner ear was removed from the head of the mouse, a small hole was made at the top of the cochlea using a 27 gauge needle, and the semicircular canals were broken open. The holes of the inner ear were gently flushed with a 2.5% glutaraldehyde fixative solution and then postfixed overnight at 4°C. Cochlear specimens were prepared by removing the stria vascularis, Reissner's membrane, and tectorial membrane. The specimens were washed three times in 0.1 M phosphate buffer (pH 7.4) for 15 min and immersed in a 1% (w/v) OsO_4 solution for 1 h at 4°C. They were dehydrated in a graded ethanol series and transferred to t-butyl alcohol. The samples were dried in a freeze dryer (Hitachi ES-2020, Hitachi High-Tech Fielding Corporation, Tokyo, Japan), coated with osmium tetroxide using an osmium plasma coater (NL-OPC80; Nippon Laser and Electronics Laboratory, Nagoya, Japan), and then examined using a Hitachi S-4800 field emission scanning electron microscope at an accelerating voltage of 10 kV.

Statistical analysis

All results are presented as the mean ± standard deviation (SD). Differences among multiple groups were analyzed by a one-way ANOVA with the Tukey post hoc multiple comparison test. The two groups were compared using a Student's *t*-test. GraphPad Prism 5 (GraphPad, San Diego, CA, USA) was used to calculate column statistics and compute *P* values.

Results

Cdh23 mRNA and CDH23 protein expression in the cochleae of $Cdh23^{ahl/ahl}$, $Cdh23^{v\text{-}ngt/ahl}$, and $Cdh23^{v\text{-}ngt/v\text{-}ngt}$ mice

Figure 1A shows a schematic diagram of the CDH23 protein structure and the locations of the functionally null and hypomorphic mutations. $Cdh23^{v\text{-}ngt}$ results from the deletion of a single guanine at position 146 in the coding region of *Cdh23* [34]. This mutation leads to a frameshift, the most severe of which within the $Cdh23^{v}$ allele series is a truncated protein that lacks all 27 EC domains as well as the transmembrane and intracellular domains [19]. In contrast, the $Cdh23^{ahl}$ mutation is a synonymous mutation. However, this mutation causes exon 7 to be skipped, leading to an in-frame deletion within the EC3 domain [26].

We hypothesized that the $Cdh23^{v\text{-}ngt}$ mutation would cause decreased expression of *Cdh23* in $Cdh23^{v\text{-}ngt}$ mice because some frameshifts lead to functional inactivation through rapid mRNA degradation. Therefore, we carried out a semiquantitative RT-PCR analysis to examine the effect of the $Cdh23^{v\text{-}ngt}$ mutation on *Cdh23* expression using RNA isolated from the cochleae of $Cdh23^{+/+}$ (C3H/HeN, 753G), $Cdh23^{ahl/ahl}$ homozygous, $Cdh23^{v\text{-}ngt/ahl}$ compound heterozygous, and $Cdh23^{v\text{-}ngt/v\text{-}ngt}$ homozygous mice. As expected, most products were not detectable in the $Cdh23^{v\text{-}ngt/v\text{-}ngt}$ homozygote, but a faint signal was detected in the lower, 267 bp, band (Fig. 1B). In the $Cdh23^{ahl/ahl}$ homozygote, an alternative exon was spliced into the mature mRNA, as previously described [26]. Notably, the transcript levels of *Cdh23* were markedly reduced in the $Cdh23^{v\text{-}ngt/ahl}$ compound heterozygous cochlea compared with the $Cdh23^{ahl/ahl}$ cochlea. To confirm and quantify the reduction in *Cdh23* in the $Cdh23^{v\text{-}ngt/ahl}$ compound heterozygous and $Cdh23^{v\text{-}ngt/v\text{-}ngt}$ homozygous mice, we performed real-time RT-PCR analysis. Although quantification was difficult because *Cdh23* expression levels were quite low, even when using several primer sets, the relative abundances of *Cdh23* transcripts in the cochleae of $Cdh23^{ahl/ahl}$, $Cdh23^{v\text{-}ngt/ahl}$, and $Cdh23^{v\text{-}ngt/v\text{-}ngt}$ mice were approximately 72.1, 52.5 and 31.5% of the levels of $Cdh23^{+/+}$ mice, respectively (Fig. 1C).

To confirm the predicted corresponding reduction in CDH23 protein levels in $Cdh23^{v\text{-}ngt/ahl}$ heterozygous mice, we performed immunoblot and immunohistochemical analyses using a rabbit polyclonal anti-CDH23 antibody. We did not detect a band specific to CDH23 in protein extracts from the inner ear in immunoblot assays. We did, however, observe immunofluorescence for CDH23 in the stereocilia, as reported in previous immunohistochemical studies. However, this signal was not detectable in the stereocilia of $Cdh23^{v\text{-}ngt/v\text{-}ngt}$ homozy-

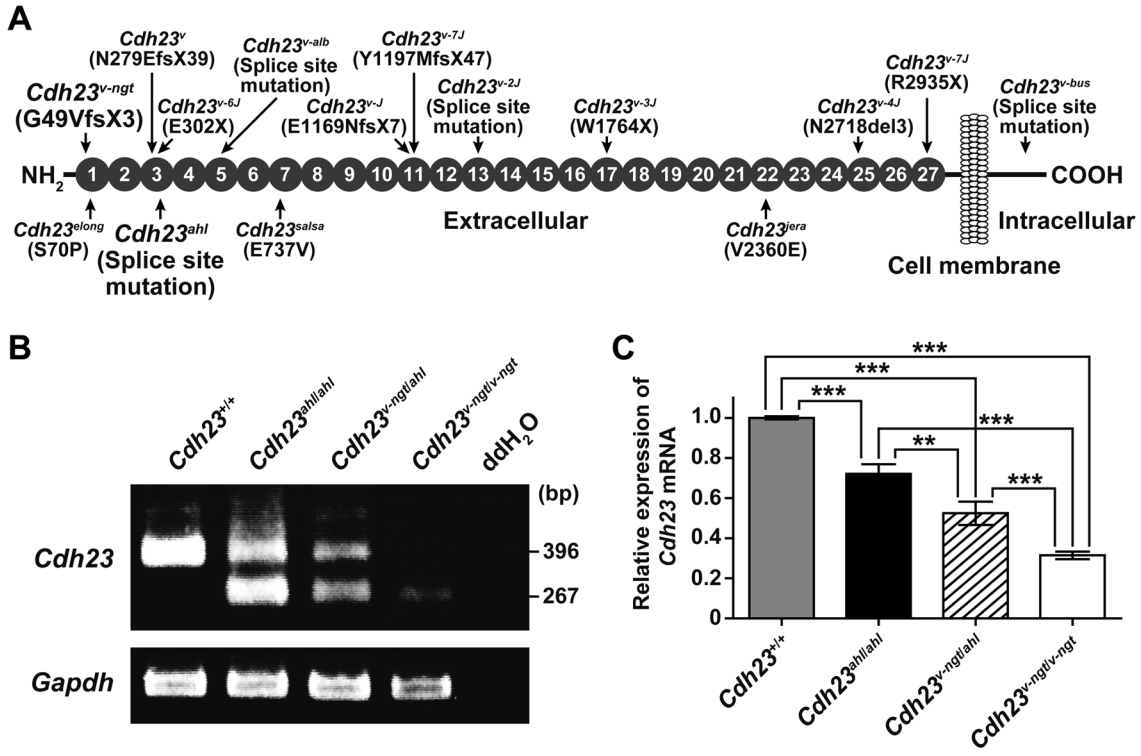

Fig. 1. *Cdh23* expression in hypomorphic *Cdh23*$^{v\text{-}ngt/v\text{-}ngt}$ homozygous, *Cdh23*$^{v\text{-}ngt/ahl}$ compound heterozygous, and null *Cdh23*$^{v\text{-}ngt/v\text{-}ngt}$ homozygous mice. (A) Schematic diagram of the CDH23 protein structure showing the locations (arrows) of the functionally null (top) and hypomorphic (bottom) mutations (modified from Manji *et al.* [13]). Gray circles indicate the extracellular cadherin repeats (ECs). (B) Semiquantitative RT-PCR analysis of *Cdh23* expression in the cochleae of *Cdh23*$^{+/+}$, *Cdh23*$^{ahl/ahl}$, *Cdh23*$^{v\text{-}ngt/ahl}$, and *Cdh23*$^{v\text{-}ngt/v\text{-}ngt}$ mice at 1 month of age. The upper panel shows 396 bp and 267 bp RT-PCR products from *Cdh23*-specific primers located in exons 6 and 8, respectively. Smaller bands (129 bp), corresponding to transcripts in which exon 7 was skipped, were amplified in cDNA samples isolated from *Cdh23*^{753A} mice. The integrity of the cDNA was confirmed using a Gapdh control band (bottom panel). (C) Relative levels of *Cdh23* mRNA in the cochleae of *Cdh23*$^{+/+}$, *Cdh23*$^{ahl/ahl}$, *Cdh23*$^{v\text{-}ngt/ahl}$, and *Cdh23*$^{v\text{-}ngt/v\text{-}ngt}$ mice at 1 month of age. *Cdh23* mRNA expression was measured by real-time RT-PCR analysis using primer set D (Supplementary Table 1: refer to J-STAGE at https://www.jstage.jst.go.jp/browse/expanim). The expression levels in *Cdh23*$^{+/+}$ mice were assigned an arbitrary value of 1 for comparative purposes. $^{**}P \leq 0.01$ and $^{***}P \leq 0.001$.

gous mice (Fig. 2, Supplementary Fig. 1A: refer to J-STAGE at https://www.jstage.jst.go.jp/browse/expanim) [13, 16, 17, 20, 29, 30]. The immunofluorescence was abundant and localized near the tip of the stereocilia on hair cells from both the *Cdh23*$^{ahl/ahl}$ homozygote and the *Cdh23*$^{v\text{-}ngt/ahl}$ heterozygote at 1 week of age (Fig. 2A). By 1 month of age, CDH23 immunofluorescence became progressively lower at the stereocilia tips, and only faint signals were detected in the outer hair cells (OHC) and inner hair cells (IHC) of *Cdh23*$^{ahl/ahl}$ and *Cdh23*$^{v\text{-}ngt/ahl}$ mice (Fig. 2B, Supplementary Fig. 1B). In addition, we had hypothesized that the expression of CDH23 in *Cdh23*$^{v\text{-}ngt/ahl}$ mice would be lower than that of *Cdh23*$^{ahl/ahl}$ mice at both 1 week and 1 month of age. As the CDH23 localization patterns were identical in the *Cdh23*$^{ahl/ahl}$ and *Cdh23*$^{v\text{-}ngt/ahl}$ mice, quantitative immunohistochemistry was performed to measure CDH23 protein expression levels in *Cdh23*$^{ahl/ahl}$ and *Cdh23*$^{v\text{-}ngt/ahl}$ mice. We quantified the immunofluorescence in the OHCs because the background was high in the IHCs. The difference at the protein level was statistically significant: CDH23 was 74.6% and 32.8% less abundant in *Cdh23*$^{v\text{-}ngt/ahl}$ OHCs at 1 week and 1 month of age, respectively, relative to *Cdh23*$^{ahl/ahl}$ OHCs ($P \leq 0.001$, Fig. 2C).

Evaluation of vestibular function and hearing abilities of Cdh23$^{ahl/ahl}$*, Cdh23*$^{v\text{-}ngt/ahl}$*, and Cdh23*$^{v\text{-}ngt/v\text{-}ngt}$ *mice*

Although the *Cdh23*$^{v\text{-}ngt/v\text{-}ngt}$ homozygous mice exhibited shaker/waltzer behavior, the *Cdh23*$^{v\text{-}ngt/ahl}$ compound heterozygous mice appeared normal. To determine

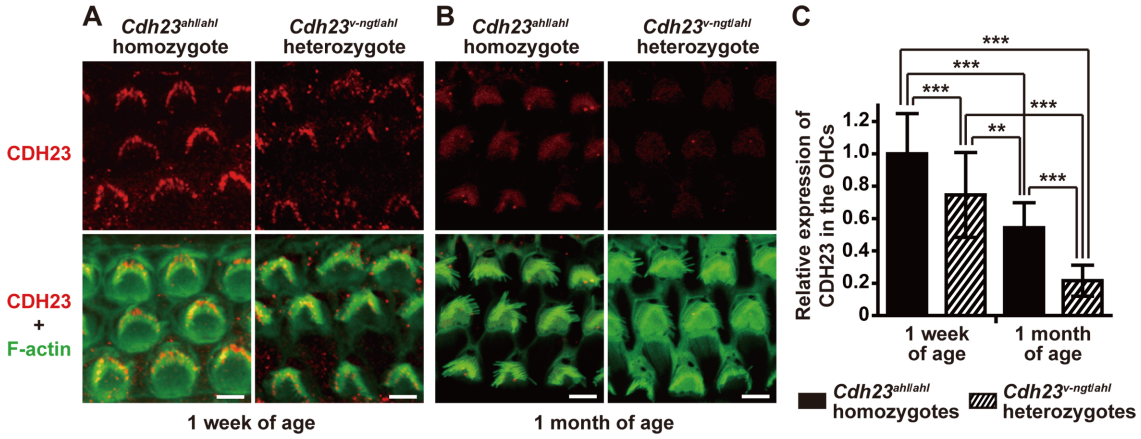

Fig. 2. Expression analysis of CDH23 protein in hair cells from hypomorphic *Cdh23*$^{ahl/ahl}$ homozygous and *Cdh23*$^{v\text{-}ngt/ahl}$ compound heterozygous mice. (A, B) Immunofluorescence labeling of CDH23 (top) and merged images (bottom) of CDH23 and F-actin (phalloidin staining; green) in stereocilia of OHCs from *Cdh23*$^{ahl/ahl}$ (left) and *Cdh23*$^{v\text{-}ngt/ahl}$ (right) mice at 1 week and 1 month of age. Scale bar=5 μm. (C). Quantification of CDH23 intensity in *Cdh23*$^{ahl/ahl}$ and *Cdh23*$^{v\text{-}ngt/ahl}$ mice at 1 week and 1 month of age. The values shown in each graph indicate the mean relative expression levels and the SDs of triplicate OHCs (n=30). **P≤0.01 and ***P≤0.001.

whether *Cdh23*$^{v\text{-}ngt/ahl}$ mice had normal vestibular function, we performed open-field behavior tests and compared phenotypes among the *Cdh23*$^{ahl/ahl}$, *Cdh23*$^{v\text{-}ngt/ahl}$, and *Cdh23*$^{v\text{-}ngt/v\text{-}ngt}$ mice. Video surveillance revealed circling and hyperactive behavior in *Cdh23*$^{v\text{-}ngt/v\text{-}ngt}$ mice (Fig. 3A); the mice traveled a long distance at high speed in the open field, and an increased number of turns were counted (Fig. 3B). In contrast, the *Cdh23*$^{v\text{-}ngt/ahl}$ compound heterozygous mice did not circle, and the distance traveled and average speeds were approximately 14% and 53%, respectively, of those of the other mice. This behavioral phenotype was similar to that of the *Cdh23*$^{ahl/ahl}$ mice and did not change at 10 months of age (Fig. 3A, B). Moreover, the morphology of the stereocilia bundles in the vestibule of *Cdh23*$^{v\text{-}ngt/ahl}$ mice was normal and similar to that of the *Cdh23*$^{ahl/ahl}$ mice, whereas *Cdh23*$^{v\text{-}ngt/v\text{-}ngt}$ mice lacked the normal staircase configuration (Fig. 3C). These results indicate that the vestibular function of *Cdh23*$^{v\text{-}ngt/ahl}$ compound heterozygous mice is likely to be normal and maintained throughout life.

Next, hearing was tested using ABRs evoked by tone-pip stimuli at 8 and 32 kHz at 1 and 5 months of age, respectively, for *Cdh23*$^{ahl/ahl}$, *Cdh23*$^{v\text{-}ngt/ahl}$, and *Cdh23*$^{v\text{-}ngt/v\text{-}ngt}$ mice. The presence of measurable thresholds at 1 month of age for *Cdh23* $^{ahl/ahl}$ and *Cdh23*$^{v\text{-}ngt/ahl}$ mice allowed us to determine the latency peak response for peaks I-V and I-IV at 8 kHz and 32 kHz, respectively (Fig. 4A). Even at the highest intensity (101 dB SPL at 8 kHz and 105 dB SPL at 32 kHz), the *Cdh23*$^{v\text{-}ngt/v\text{-}ngt}$ mice showed no ABR. Although similar patterns of wave amplitudes, latencies, and peak thresholds were observed in the *Cdh23*$^{ahl/ahl}$ and *Cdh23*$^{v\text{-}ngt/ahl}$ mice, most *Cdh23*$^{v\text{-}ngt/ahl}$ mice showed reductions in the peak amplitudes (Fig. 4A). At 5 months of age, the amplitudes of the peaks were significantly reduced in *Cdh23*$^{v\text{-}ngt/ahl}$ mice compared with *Cdh23*$^{ahl/ahl}$ mice (Fig. 4B). However, the ABR waveforms at 8 kHz recorded in the *Cdh23*$^{v\text{-}ngt/ahl}$ mice varied by individual. Interestingly, distinct waveforms were recorded for the left and right ears in the same *Cdh23*$^{v\text{-}ngt/ahl}$ mouse (Fig. 4B). In contrast, our evaluation of ABRs at 32 kHz demonstrated that most *Cdh23*$^{v\text{-}ngt/ahl}$ mice were profoundly hearing impaired by 5 months of age (Fig. 4B). We next determined the ABR thresholds for tone-pip stimuli at 4, 8, 16 and 32 kHz in *Cdh23*$^{ahl/ahl}$ and *Cdh23*$^{v\text{-}ngt/ahl}$ mice at 1–12 months of age at 1 month intervals (Fig. 5). This analysis revealed a clear increase in ABR thresholds in the *Cdh23*$^{v\text{-}ngt/ahl}$ mice. For ABR thresholds in response to stimuli at 4 kHz, mean differences were detected between *Cdh23*$^{ahl/ahl}$ and *Cdh23*$^{v\text{-}ngt/ahl}$ mice at several time points, but they did not reach statistical significance. A significant difference in ABR thresholds at 8 kHz was first observed between *Cdh23*$^{v\text{-}ngt/ahl}$ and *Cdh23*$^{ahl/ahl}$ mice at 4 months of age, and the hearing impairment increased in severity in an age-dependent manner. Mean ABR thresholds at 16 and 32 kHz were also significantly increased in *Cdh23*$^{v\text{-}ngt/ahl}$ mice and rapidly reached a level indicative of profound hearing impairment. These results suggest

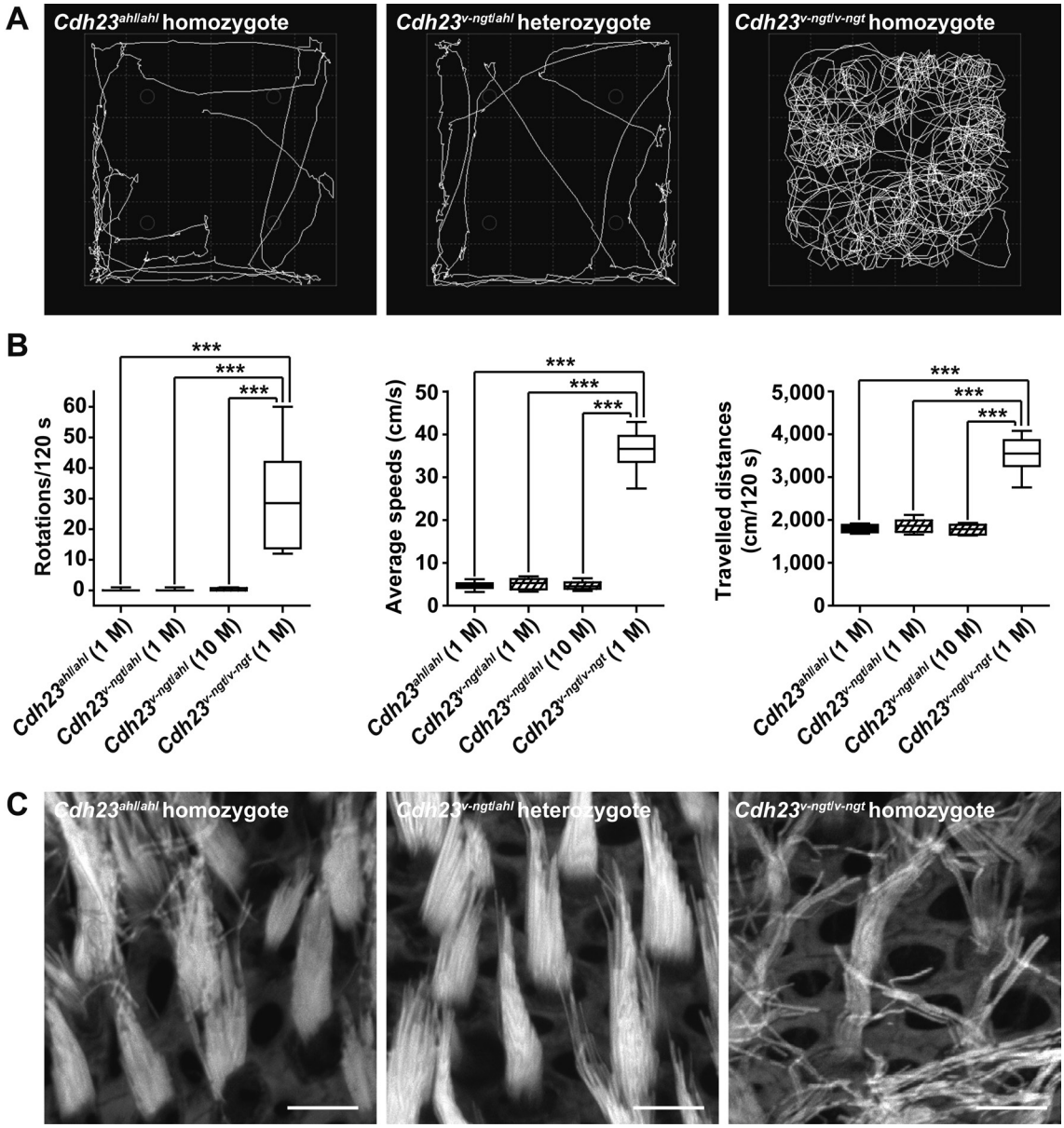

Fig. 3. Vestibular function of *Cdh23*$^{ahl/ahl}$, *Cdh23*$^{v\text{-}ngt/ahl}$, and *Cdh23*$^{v\text{-}ngt/v\text{-}ngt}$ mice. (A) Representative open-field pathway traces (white lines) from 1-month-old mice of each *Cdh23* genotype. (B) Quantitation of the number of rotations in 120 s (left), average movement speed (middle), and total traveled distance (right) from 16 mice of each *Cdh23* genotype at 1 month of age and 16 *Cdh23*$^{v\text{-}ngt/ahl}$ mice at 10 months of age. ***$P \leq 0.001$. (C) Stereociliary phenotypes of vestibular hair cells from 1-month-old mice of each *Cdh23* genotype. The utricle of the vestibular labyrinth was stained with phalloidin. Scale bar=5 μm.

that *Cdh23*$^{v\text{-}ngt/ahl}$ mice exhibit an early-onset and progressive hearing impairment that is more severe in response to high-frequency stimuli (Figs. 4 and 5).

Morphological changes in stereocilia by the combination of Cdh23 mutant alleles

The rapid early-onset hearing impairment observed in the *Cdh23*$^{v\text{-}ngt/ahl}$ compound heterozygous mice suggested that degeneration of cochlear hair cells may occur at relatively young ages. Mice expressing *Cdh23* mutant alleles share common defects in stereocilia development and the maintenance of hair cells [8, 11, 17–19, 29, 34]. We therefore examined both IHCs and OHCs from organs of Corti in *Cdh23*$^{v\text{-}ngt/ahl}$ mice at 1–10 months of

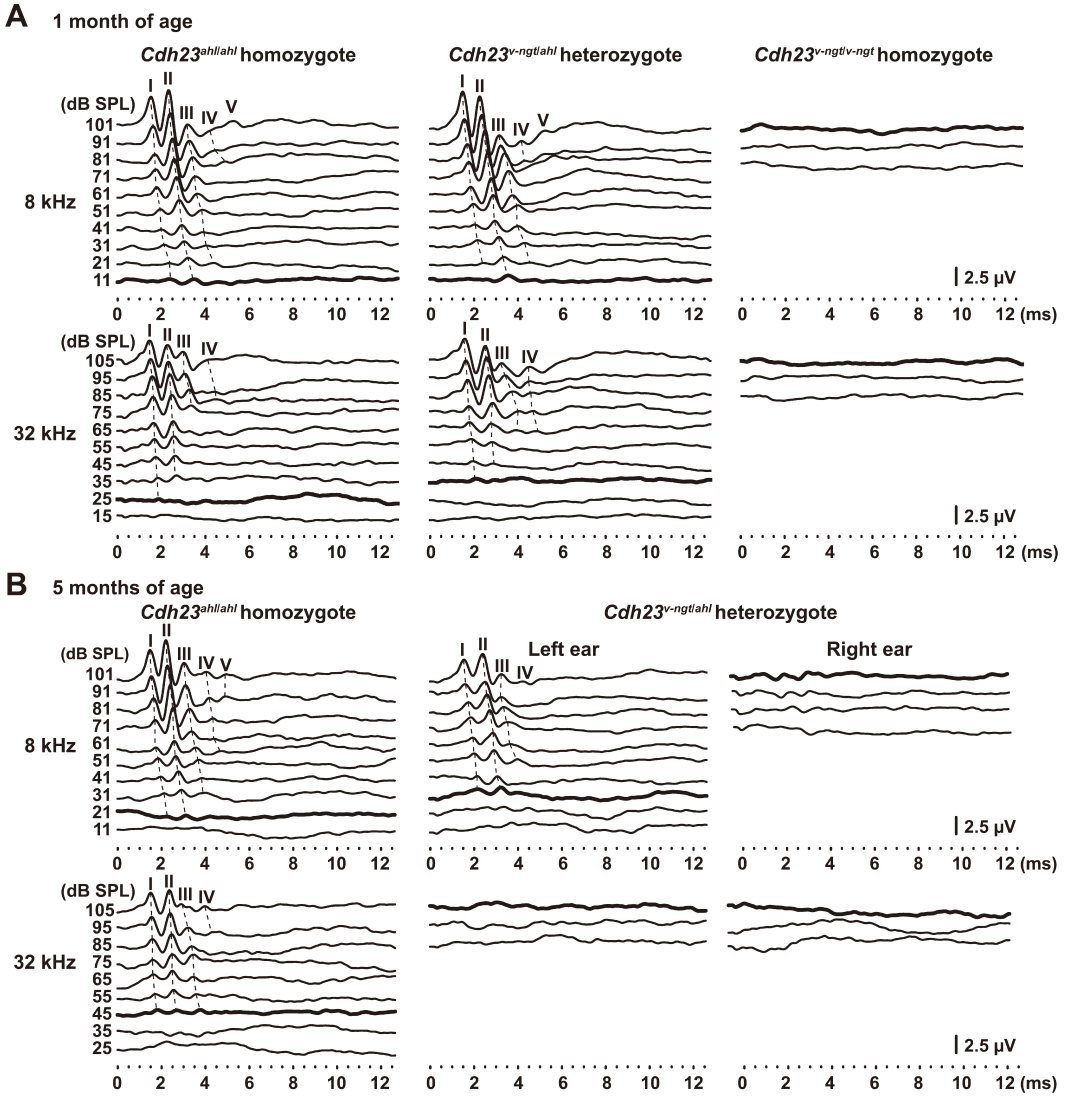

Fig. 4. ABR waveforms were recorded for hypomorphic *Cdh23*$^{ahl/ahl}$ homozygous, *Cdh23*$^{v\text{-}ngt/ahl}$ compound heterozygous, and null *Cdh23*$^{v\text{-}ngt/v\text{-}ngt}$ homozygote mice. The waveforms represent the ABR in response to the intensities of tone pip stimuli decreasing from 101 to 11 dB SPL at 8 kHz and from 105 to 15 dB SPL at 32 kHz. Bold lines represent the thresholds detected. The locations of peaks I-V are indicated on the dotted lines. (A) Representative ABR waveforms at 8 and 32 kHz from *Cdh23*$^{ahl/ahl}$, *Cdh23*$^{v\text{-}ngt/ahl}$, and *Cdh23*$^{v\text{-}ngt/v\text{-}ngt}$ mice at 1 month of age. (B) ABR waveforms at 8 and 32 kHz from *Cdh23*$^{ahl/ahl}$ and *Cdh23*$^{v\text{-}ngt/ahl}$ mice at 5 months of age. The waveforms of the *Cdh23*$^{v\text{-}ngt/ahl}$ mouse were recorded from the left and right ear of the same mouse.

age via SEM to better understand the structure-function relationship in *Cdh23*$^{v\text{-}ngt/ahl}$ compound heterozygous mice. Figure 6 shows the stereociliary morphology of *Cdh23*$^{v\text{-}ngt/v\text{-}ngt}$ homozygous and *Cdh23*$^{v\text{-}ngt/ahl}$ compound heterozygous mice at 1 month of age. In *Cdh23*$^{v\text{-}ngt/v\text{-}ngt}$ mice, the OHC stereocilia were severely disrupted (Fig. 6A, C), whereas the IHC stereocilia were either missing or fused (Fig. 6E). By contrast, in *Cdh23*$^{v\text{-}ngt/ahl}$ mice, the stereocilia displayed "V"-shaped and staircase-like configurations on the OHCs (Fig. 6B, D) and crescent- and staircase-shaped configurations on IHCs (Fig. 6F) in the apex and middle area of the cochlea, corresponding to hearing at 8–16 kHz [22]. However, we found that stereocilia on IHCs at the base of the cochlea, corresponding to hearing at 32 kHz [22], began to show signs of disorganization by 1 month of age; a few OHCs were missing bundles (Fig. 6G), and disruptions, including splits in the bundle, were also observed (Fig. 6H). The stereocilia became progressively more disrupted in *Cdh23*$^{v\text{-}ngt/ahl}$ mice with increasing age. At 4 months of

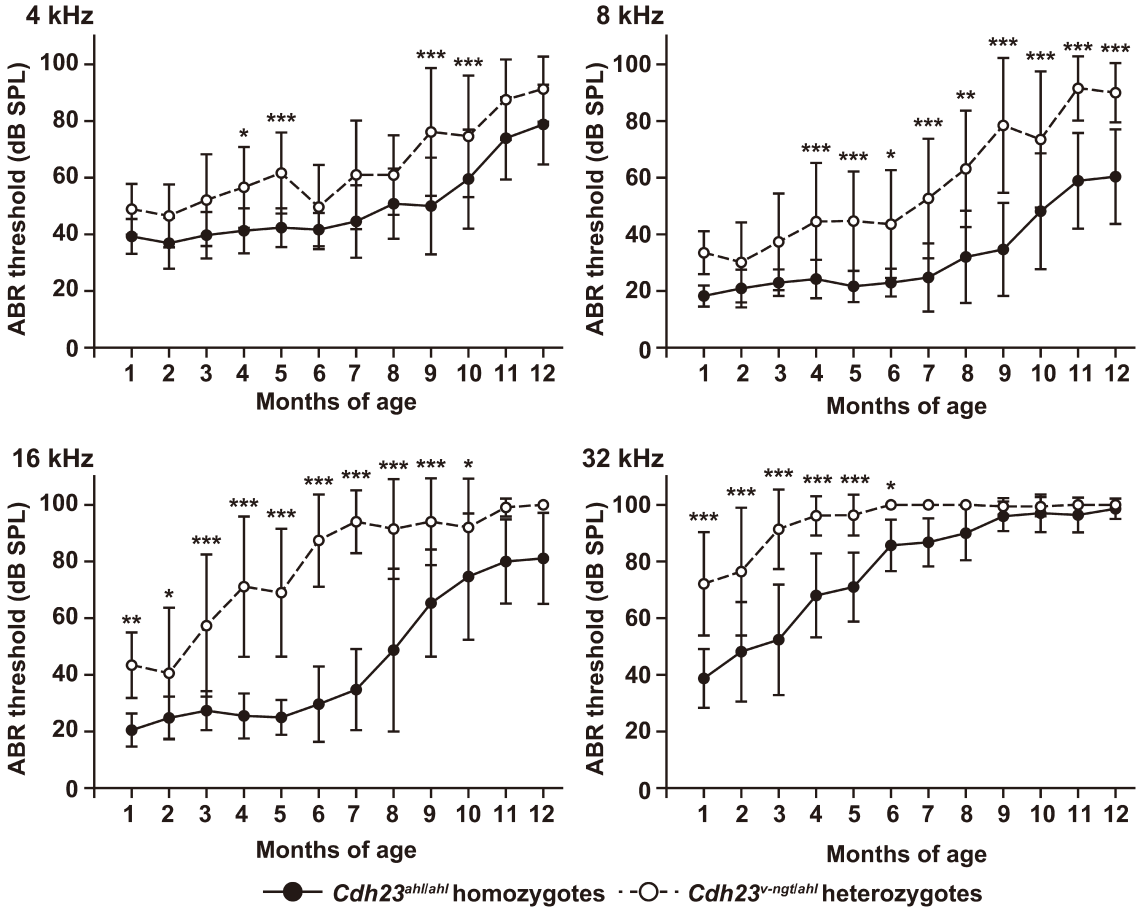

Fig. 5. Comparison of age-related hearing loss in hypomorphic *Cdh23*$^{ahl/ahl}$ homozygous and compound *Cdh23*$^{v\text{-}ngt/ahl}$ heterozygous mice. The means (black and white circles) and SDs (error bars) of ABR threshold measurements for 4, 8, 16, and 32 kHz stimuli are shown for each strain of mice at 1 to 12 months of age. The number of ears tested is listed in Supplementary Table 2: refer to J-STAGE at https://www.jstage.jst.go.jp/browse/expanim. *$P \leq 0.05$; **$P \leq 0.01$; and ***$P \leq 0.001$.

age, gaps within the ranks of stereocilia and missing bundles on OHCs were observed in the middle region of the cochlea (Fig. 7A), which detects stimuli at 16 kHz. From 4 to 7 months of age, an increasing number of OHC stereocilia were affected; most stereocilia were disrupted, and some were missing (Fig. 7B, C). This pattern of stereocilia degeneration may correlate with the time course of increased ABR thresholds at 16 kHz in *Cdh23*$^{v\text{-}ngt/ahl}$ mice (Fig. 5). By 10 months of age, the stereocilia in the apex showed severe degeneration in *Cdh23*$^{v\text{-}ngt/ahl}$ compound heterozygous mice (Fig. 7D, E). Moreover, we found elongated tip links (Fig. 7F) on the stereocilia of OHCs and fused bundles (Fig. 7G) on IHCs in *Cdh23*$^{v\text{-}ngt/ahl}$ mice at this stage. In contrast, the phenotypes of stereocilia on OHCs from the apex of the cochlea were normal in *Cdh23*$^{ahl/ahl}$ mice at 10 months of age (Fig. 7H). Here, stereocilia degeneration occurred at a much older age (Fig. 7I). These results suggest that compound heterozygotes of the null *Cdh23*$^{v\text{-}ngt}$ and hypomorphic *Cdh23*^{ahl} alleles experience a rapid hearing loss followed by degeneration of the stereocilia.

Discussion

Fifteen *Cdh23* mutations have been identified in mice, all of which show a recessive phenotype. Eleven of the 15 alleles have been classified as *Cdh23*^{v}, which confers a phenotype consisting of profound hearing loss from birth and abnormal shaker/waltzer behavior associated with severe stereocilia disorganization (Figs. 3 and 6) [7, 8, 34, 37, 39]. Within these *Cdh23*^{v} mutations, three (*Cdh23*$^{v\text{-}3J}$, *Cdh23*$^{v\text{-}5J}$, and *Cdh23*$^{v\text{-}6J}$) are nonsense muta-

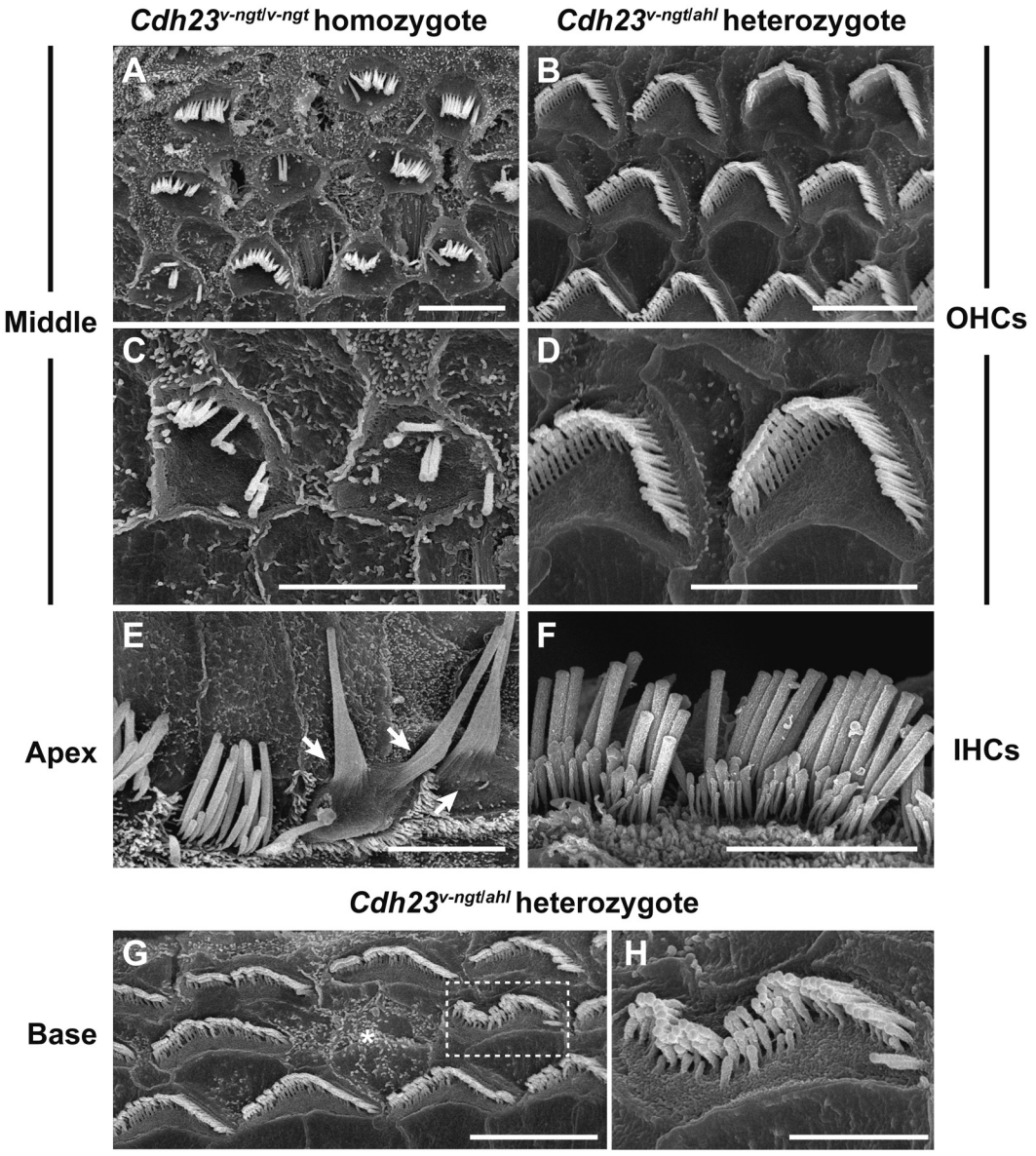

Fig. 6. Stereocilia phenotypes in *Cdh23*$^{v\text{-}ngt/ahl}$ heterozygous and *Cdh23*$^{v\text{-}ngt/v\text{-}ngt}$ homozygous mice at 1 month of age. SEM images showing the stereocilia of cochlear hair cells in *Cdh23*$^{v\text{-}ngt/v\text{-}ngt}$ (A, C, E) and *Cdh23*$^{v\text{-}ngt/ahl}$ (B, D, F, G, H) mice. (A–D) Stereociliary morphology of outer hair cells (OHCs) from the middle area of the cochlea in *Cdh23*$^{v\text{-}ngt/v\text{-}ngt}$ and *Cdh23*$^{v\text{-}ngt/ahl}$ mice. Highly magnified images are shown in C and D. (E, F) Stereociliary morphology of inner hair cells (IHCs) from the apical area in *Cdh23*$^{v\text{-}ngt/v\text{-}ngt}$ and *Cdh23*$^{v\text{-}ngt/ahl}$ mice. Arrows indicate fused stereociliary bundles in *Cdh23*$^{v\text{-}ngt/v\text{-}ngt}$ mice (E). (G, H) Stereociliary morphology of OHCs from the basal turn of the cochlea in *Cdh23*$^{v\text{-}ngt/ahl}$ mice. Asterisks indicate OHCs with missing bundles. A highly magnified image of stereocilia in the dotted box in G is shown in H. Scale bars=5 μm (A-G) and 2 μm (H).

tions, and five (*Cdh23*$^{v\text{-}ngt}$, *Cdh23*^{v}, *Cdh23*$^{v\text{-}alb}$, *Cdh23*$^{v\text{-}J}$, and *Cdh23*$^{v\text{-}7J}$) are predicted to cause frameshift mutations that result in premature truncation of the peptide by generating stop codons in the ECs (Fig. 1A) [7, 8, 34, 37]. These truncated peptides lack several ECs, the transmembrane domain, and the short intracellular domain and are presumably functionally null (Fig. 1A). *Cdh23*$^{v\text{-}2J}$ and *Cdh23*$^{v\text{-}bus}$ are splice site mutations that alter the wild-type splice site and introduce a premature stop codon, although a small amount of normally processed transcript can be detected in the cDNA [7, 39]. The *Cdh23*$^{v\text{-}4J}$ mutation carries a 9 bp in-frame deletion that

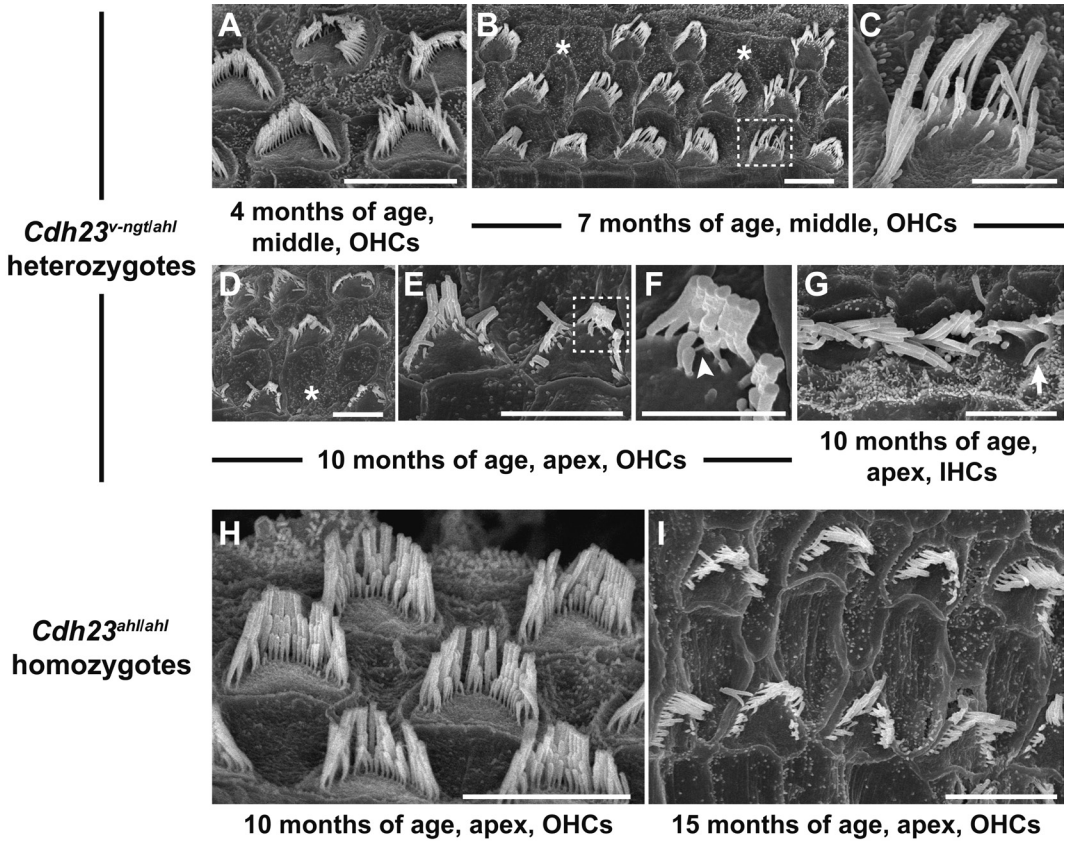

Fig. 7. Age-related degeneration of cochlear hair cells in *Cdh23*$^{v\text{-}ngt/ahl}$ heterozygous mice. SEM micrographs show the stereociliary phenotypes of compound *Cdh23*$^{v\text{-}ngt/ahl}$ heterozygous (A–G) and hypomorphic *Cdh23*$^{ahl/ahl}$ homozygous (H, I) mice. (A–G) Stereociliary morphology of OHCs (A-F) and IHCs (G) in *Cdh23*$^{v\text{-}ngt/ahl}$ mice at 4, 7 and 10 months of age. Asterisks indicate OHCs with missing bundles (B, D). Highly magnified images of stereocilia in the dotted boxes in B and E are shown in C and F, respectively. The arrowhead (F) indicates an elongated tip link, and the arrow (G) indicates a fused stereocilia bundle. (H, I) Stereociliary morphology of OHCs in *Cdh23*$^{ahl/ahl}$ mice at 10 and 15 months of age. Scale bars=5 μm (A, B, D, E, G–I) and 2 μm (C, F).

eliminates three amino acids from EC25 [8]. As these *Cdh23*$^{v\text{-}2J}$, *Cdh23*$^{v\text{-}bus}$, and *Cdh23*$^{v\text{-}4J}$ mutations confer *v* phenotypes similar to those of the functionally null alleles, they are also assumed to be loss-of-function mutations. In contrast, mice with missense mutations in the ECs, *Cdh23*^{elong}, *Cdh23*^{salsa}, and *Cdh23*^{jera}, which were identified through N-ethyl-N-nitrosourea (ENU) mutagenesis screens, exhibited early-onset hearing loss without vestibular dysfunction. Unlike the *Cdh23*^{v} alleles, these mutations are hypomorphic and associated with progressive loss of the tip links, but the development of the stereocilia bundles is unaffected [18, 19, 29]. *Cdh23*^{ahl} is another hypomorphic mutation that results in the expression of a transcript lacking exon 7 (Fig. 1B). This allele causes AHL without vestibular dysfunction (Figs. 3 and 5) [26]. In this study, we produced mice carrying the *Cdh23*$^{v\text{-}ngt}$ null allele in combination with the hypomorphic *Cdh23*^{ahl} allele and analyzed their hearing phenotypes. The results showed that *Cdh23*$^{v\text{-}ngt/ahl}$ mice exhibit a hearing loss phenotype encompassing high to low frequencies, which is typical of AHL. The onset of hearing loss was earlier than in *Cdh23*$^{ahl/ahl}$ homozygous mice (Figs. 4 and 5). Moreover, we found that the rapid hearing loss of *Cdh23*$^{v\text{-}ngt/ahl}$ compound heterozygous mice is associated with age-related degeneration of the stereocilia in the cochlear hair cells.

In a previous study, Holme and Steel [11] reported that mice heterozygous for one of the functionally null *Cdh23*^{v} mutations show early-onset progressive hearing loss, similar to our findings for the *Cdh23*$^{v\text{-}ngt/ahl}$ heterozygous mice. However, the study of Holme and Steel did not confirm that the expression of early-onset progressive hearing loss is associated with a compound heterozygous state comprised of a functionally null allele

and a hypomorphic allele because the authors analyzed *Cdh23*^{v} heterozygous mice on mixed genetic backgrounds that were 50% CBA/Ca and 50% BS, with some BALB/c [11], and inbred mice are known to have several other AHL susceptibility loci [15, 25]. In our study, to avoid effects from modifier genes on other chromosomes, we produced congenic mice by crossing the *Cdh23*$^{v\text{-}ngt}$ null allele with the hypomorphic *Cdh23*^{ahl} allele onto the C57BL/6J background. Our findings confirm that expression of early-onset progressive hearing loss is more likely in a compound heterozygote of a functionally null and a hypomorphic allele of *Cdh23*.

By contrast, mice heterozygous for the purported loss-of-function *Cdh23*$^{v\text{-}2J}$ allele did not exhibit early-onset AHL and showed similar hearing patterns as *Cdh23*$^{ahl/ahl}$ mice [40, 41]. The genetic background of mice carrying the *Cdh23*$^{v\text{-}2J}$ allele includes C57BL/6J, similar to that of mice carrying the *Cdh23*$^{v\text{-}ngt}$ allele, and the *Cdh23* genotype in this heterozygote is predicted to be *v-2J*/*ahl* [40, 41]. These data may indicate that the *Cdh23*$^{v\text{-}2J}$ mutation is a loss-of-function mutation and that *Cdh23*$^{v\text{-}2J/ahl}$ does not represent a compound heterozygote between a null allele and a hypomorphic allele; low levels of wild-type CDH23 in the tip links of the stereocilia may have allowed the mice to retain the ability to hear for a long time.

In wild-type mice, CDH23 is expressed in kinocilial links as well as the transient links that develop at early stages [16, 20, 30]. Kinocilial links and transient links are important for hair bundle development because cohesive forces applied early are necessary for the normal formation of stereocilia bundles [14, 17, 24]. Mice carrying functionally null alleles of CDH23 (*Cdh23*^{v}) exhibit displacement of the kinocilia as well as fragmentation and irregular stereocilia length in both cochlear and vestibular hair cells [7, 17, 34]. These phenotypes could result from defects in the transient links. By contrast, the *Cdh23*$^{v\text{-}ngt/ahl}$ mice showed normal stereocilia development in both cochlear and vestibular hair cells (Fig. 6). Moreover, we detected normal localization of CDH23 lacking exon 7 in the stereocilia of *Cdh23*$^{v\text{-}ngt/ahl}$ mice, but its expression level was lower in *Cdh23*$^{v\text{-}ngt/ahl}$ heterozygous mice than in *Cdh23*$^{ahl/ahl}$ homozygous mice probably due to the gene dosage effect (Fig. 2). These results may suggest that stereocilia development is not affected by reductions in either CDH23 or CDH23 lacking exon 7 and that the presence of CDH23 in the stereocilia is more important than expression level for organizing the stereocilia.

In mature stereocilia of vertebrates, CDH23 is localized to the tip link, which is thought to gate the mechanoelectrical transduction (MET) channels that convey mechanical forces such as sound and gravity [10, 13, 30, 31, 38]. The tip links are formed by a tetramer of CDH23 and another cadherin, protocadherin 15 (PCDH15); the interaction between the two cadherins is important to maintain the morphology and tension of the tip links [13, 32]. The clear increase in ABR thresholds observed in *Cdh23*$^{v\text{-}ngt/ahl}$ mice at 1–3 months of age could therefore be explained by abnormal MET gating associated with reduced tension of the tip links caused by the reduced amount of CDH23 lacking exon 7 but not by the reduced amount of normal CDH23 (Figs. 1, 2 and 5). Moreover, we found that the rapid hearing loss in *Cdh23*$^{v\text{-}ngt/ahl}$ heterozygous mice was associated with age-related degeneration of the stereocilia (Fig. 7). Our data may suggest that maintenance of tip links is a sensitive aging process affected by the reduced amount of CDH23 lacking exon 7 in *Cdh23*$^{v\text{-}ngt/ahl}$ heterozygous mice.

In humans, null mutations in *CDH23* cause an autosomal recessive disorder called Usher syndrome type ID (USH1D) [4]. USH1 is an autosomal recessive disorder characterized by congenital deafness, vestibular dysfunction, and prepubertal onset of progressive retinitis pigmentosa (RP) [27]. Based on the severity and progression of hearing loss, the age at onset of RP, and the presence or absence of vestibular impairment, USH is categorized into three types, the most severe of which is USH1. Mutations in *CDH23* cause not only USH1 but also recessive non-syndromic hearing loss (DFNB12; deafness, autosomal recessive 12) without vestibular dysfunction or RP [5]. Mutations predicted to truncate CDH23 in the extracellular domains typically cause USH1, whereas missense mutations predicted to change only single amino acids are commonly associated with DFNB12. The mutation spectrum suggests that functionally null alleles cause USH1, whereas hypomorphic alleles lead to less severe forms of the disease [4, 5, 23]. Some compound heterozygotes with one functionally null allele and one hypomorphic allele of *CDH23* have an Usher phenotype [1]. In contrast, a recent study reported that one hypomorphic *CDH23* allele in trans configuration to a null *CDH23* allele preserves vision and balance in deaf individuals [28]. Moreover, no allelic variants of *CDH23* that cause RP or vestibular dysfunction with normal hearing have been reported [1, 4, 5, 28]. These

results indicate that hypomorphic *CDH23* alleles are phenotypically dominant to null *CDH23* alleles and that hearing is more affected by *CDH23* mutations than vision or vestibular function. We showed that the vestibular function of *Cdh23*$^{v\text{-}ngt/ahl}$ compound heterozygous mice was normal (Fig. 3), though the mice exhibited early-onset hearing loss (Figs. 4 and 5). Although gross physiological abnormalities in the retina have not been detected in the *Cdh23* mutant mice, phenotypic and molecular genetic analyses of these functionally null, hypomorphic, and compound heterozygous mice could provide the basis necessary to elucidate the molecular mechanisms of the genotype-phenotype correlations and to distinguish between the cochlea and vestibule in the development and maintenance of hair cell stereocilia.

Acknowledgments

We thank Sachi Yoshimoto, Takayuki Sugaya, and Yusuke Sakuma for technical assistance and Dr. Kazusaku Kamiya for providing us with anti-CDH23 antibody. This work was financially supported through Grants-in-Aid for Scientific Research (B, no. 20300147, and B, no. 23300160) from the Japan Society for the Promotion of Science.

References

1. Astuto, L.M., Bork, J.M., Weston, M.D., Askew, J.W., Fields, R.R., Orten, D.J., Ohliger, S.J., Riazuddin, S., Morell, R.J., Khan, S., Riazuddin, S., Kremer, H., van Hauwe, P., Moller, C.G., Cremers, C.W., Ayuso, C., Heckenlively, J.R., Rohrschneider, K., Spandau, U., Greenberg, J., Ramesar, R., Reardon, W., Bitoun, P., Millan, J., Legge, R., Friedman, T.B., and Kimberling, W.J. 2002. *CDH23* mutation and phenotype heterogeneity: a profile of 107 diverse families with Usher syndrome and nonsyndromic deafness. *Am. J. Hum. Genet.* 71: 262–275. [Medline] [CrossRef]
2. Anagnostopoulos, A.V. 2002. A compendium of mouse knockouts with inner ear defects. *Trends. Genet.* 18: S21–S38. [Medline] [CrossRef]
3. Beck, J.A., Lloyd, S., Hafezparast, M., Lennon-Pierce, M., Eppig, J.T., Festing, M.F., and Fisher, E.M. 2000. Genealogies of mouse inbred strains. *Nat. Genet.* 24: 23–25. [Medline] [CrossRef]
4. Bolz, H., von Brederlow, B., Ramírez, A., Bryda, E.C., Kutsche, K., Nothwang, H.G., Seeliger, M., del C-Salcedó Cabrera, M., Vila, M.C., Molina, O.P., Gal, A., and Kubisch, C. 2001. Mutation of *CDH23*, encoding a new member of the cadherin gene family, causes Usher syndrome type 1D. *Nat. Genet.* 27: 108–112. [Medline] [CrossRef]
5. Bork, J.M., Peters, L.M., Riazuddin, S., Bernstein, S.L., Ahmed, Z.M., Ness, S.L., Polomeno, R., Ramesh, A., Schloss, M., Srisailpathy, C.R., Wayne, S., Bellman, S., Desmukh, D., Ahmed, Z., Khan, S.N., Kaloustian, V.M., Li, X.C., Lalwani, A., Riazuddin, S., Bitner-Glindzicz, M., Nance, W.E., Liu, X.Z., Wistow, G., Smith, R.J., Griffith, A.J., Wilcox, E.R., Friedman, T.B., and Morell, R.J. 2001. Usher syndrome 1D and nonsyndromic autosomal recessive deafness DFNB12 are caused by allelic mutations of the novel cadherin-like gene *CDH23*. *Am. J. Hum. Genet.* 68: 26–37. [Medline] [CrossRef]
6. Ding, D., McFadden, S.L., and Salvi, R.J. Cochlear hair cell densities and inner-ear staining techniques. pp. 189–204. *In*: Handbook of Mouse Auditory Research: From Behavior to Molecular Biology. (Willott J.F. ed.), CRC Press, Boca Raton, London, New York and Washington, D.C.
7. Di Palma, F., Holme, R.H., Bryda, E.C., Belyantseva, I.A., Pellegrino, R., Kachar, B., Steel, K.P., and Noben-Trauth, K. 2001. Mutations in *Cdh23*, encoding a new type of cadherin, cause stereocilia disorganization in waltzer, the mouse model for Usher syndrome type 1D. *Nat. Genet.* 27: 103–107. [Medline] [CrossRef]
8. Di Palma, F., Pellegrino, R., and Noben-Trauth, K. 2001. Genomic structure, alternative splice forms and normal and mutant alleles of cadherin 23 (*Cdh23*). *Gene* 281: 31–41. [Medline] [CrossRef]
9. Erway, L.C., Willott, J.F., Archer, J.R., and Harrison, D.E. 1993. Genetics of age-related hearing loss in mice: I. Inbred and F1 hybrid strains. *Hear. Res.* 65: 125–132. [Medline] [CrossRef]
10. Gillespie, P.G. and Müller, U. 2009. Mechanotransduction by hair cells: models, molecules, and mechanisms. *Cell* 139: 33–44. [Medline] [CrossRef]
11. Holme, R.H. and Steel, K.P. 2002. Stereocilia defects in waltzer (*Cdh23*), shaker1 (*Myo7a*) and double waltzer/shaker1 mutant mice. *Hear. Res.* 169: 13–23. [Medline] [CrossRef]
12. Johnson, K.R., Erway, L.C., Cook, S.A., Willott, J.F., and Zheng, Q.Y. 1997. A major gene affecting age-related hearing loss in C57BL/6J mice. *Hear. Res.* 114: 83–92. [Medline] [CrossRef]
13. Kazmierczak, P., Sakaguchi, H., Tokita, J., Wilson-Kubalek, E.M., Milligan, R.A., Müller, U., and Kachar, B. 2007. Cadherin 23 and protocadherin 15 interact to form tip-link filaments in sensory hair cells. *Nature* 449: 87–91. [Medline] [CrossRef]
14. Kelly, M. and Chen, P. 2007. Shaping the mammalian auditory sensory organ by the planar cell polarity pathway. *Int. J. Dev. Biol.* 51: 535–547. [Medline] [CrossRef]
15. Kikkawa, Y., Seki, Y., Okumura, K., Ohshiba, Y., Miyasaka, Y., Suzuki, S., Ozaki, M., Matsuoka, K., Noguchi, Y., and Yonekawa, H. 2012. Advantages of a mouse model for human hearing impairment. *Exp. Anim.* 61: 85–98. [Medline] [CrossRef]
16. Lagziel, A., Ahmed, Z.M., Schultz, J.M., Morell, R.J., Belyantseva, I.A., and Friedman, T.B. 2005. Spatiotemporal pattern and isoforms of cadherin 23 in wild type and *waltzer* mice during inner ear hair cell development. *Dev. Biol.* 280: 295–306. [Medline] [CrossRef]

17. Lefèvre, G., Michel, V., Weil, D., Lepelletier, L., Bizard, E., Wolfrum, U., Hardelin, J.P., and Petit, C. 2008. A core cochlear phenotype in USH1 mouse mutants implicates fibrous links of the hair bundle in its cohesion, orientation and differential growth. *Development.* 135: 1427–1437. [Medline] [CrossRef]
18. Liu, S., Li, S., Zhu, H., Cheng, S., and Zheng, Q.Y. 2012. A mutation in the *cdh23* gene causes age-related hearing loss in *Cdh23* (*nmf308/nmf308*) mice. *Gene.* 499: 309–317. [Medline] [CrossRef]
19. Manji, S.S., Miller, K.A., Williams, L.H., Andreasen, L., Siboe, M., Rose, E., Bahlo, M., Kuiper, M., and Dahl, H.H. 2011. An ENU-induced mutation of *Cdh23* causes congenital hearing loss, but no vestibular dysfunction, in mice. *Am. J. Pathol.* 179: 903–914. [Medline] [CrossRef]
20. Michel, V., Goodyear, R.J., Weil, D., Marcotti, W., Perfettini, I., Wolfrum, U., Kros, C.J., Richardson, G.P., and Petit, C. 2005. Cadherin 23 is a component of the transient lateral links in the developing hair bundles of cochlear sensory cells. *Dev. Biol.* 280: 281–294. [Medline] [CrossRef]
21. Mikaelian, D.O. 1979. Development and degeneration of hearing in the C57/b16 mouse: relation of electrophysiologic responses from the round window and cochlear nucleus to cochlear anatomy and behavioral responses. *Laryngoscope* 89: 1–15. [Medline] [CrossRef]
22. Müller, M., von Hünerbein, K., Hoidis, S., and Smolders, J.W. 2005. A physiological place-frequency map of the cochlea in the CBA/J mouse. *Hear. Res.* 202: 63–73. [Medline] [CrossRef]
23. Müller, U. 2008. Cadherins and mechanotransduction by hair cells. *Curr. Opin. Cell Biol.* 20: 557–566. [Medline] [CrossRef]
24. Nayak, G.D., Ratnayaka, H.S., Goodyear, R.J., and Richardson, G.P. 2007. Development of the hair bundle and mechanotransduction. *Int. J. Dev. Biol.* 51: 597–608. [Medline] [CrossRef]
25. Noben-Trauth, K. and Johnson, K.R. 2009. Inheritance patterns of progressive hearing loss in laboratory strains of mice. *Brain Res.* 1277: 42–51. [Medline] [CrossRef]
26. Noben-Trauth, K., Zheng, Q.Y., and Johnson, K.R. 2003. Association of cadherin 23 with polygenic inheritance and genetic modification of sensorineural hearing loss. *Nat. Genet.* 35: 21–23. [Medline] [CrossRef]
27. Pan, L. and Zhang, M. 2012. Structures of usher syndrome 1 proteins and their complexes. *Physiology (Bethesda)* 27: 25–42 (Bethesda). [Medline] [CrossRef]
28. Schultz, J.M., Bhatti, R., Madeo, A.C., Turriff, A., Muskett, J.A., Zalewski, C.K., King, K.A., Ahmed, Z.M., Riazuddin, S., Ahmad, N., Hussain, Z., Qasim, M., Kahn, S.N., Meltzer, M.R., Liu, X.Z., Munisamy, M., Ghosh, M., Rehm, H.L., Tsilou, E.T., Griffith, A.J., Zein, W.M., Brewer, C.C., Riazuddin, S., and Friedman, T.B. 2011. Allelic hierarchy of *CDH23* mutations causing non-syndromic deafness DFNB12 or Usher syndrome USH1D in compound heterozygotes. *J. Med. Genet.* 48: 767–775. [Medline] [CrossRef]
29. Schwander, M., Xiong, W., Tokita, J., Lelli, A., Elledge, H.M., Kazmierczak, P., Sczaniecka, A., Kolatkar, A., Wiltshire, T., Kuhn, P., Holt, J.R., Kachar, B., Tarantino, L., and Müller, U. 2009. A mouse model for nonsyndromic deafness (DFNB12) links hearing loss to defects in tip links of mechanosensory hair cells. *Proc. Natl. Acad. Sci. USA* 106: 5252–5257. [Medline] [CrossRef]
30. Siemens, J., Lillo, C., Dumont, R.A., Reynolds, A., Williams, D.S., Gillespie, P.G., and Müller, U. 2004. Cadherin 23 is a component of the tip in hair-cell stereocilia. *Nature* 428: 950–955. [Medline] [CrossRef]
31. Söllner, C., Rauch, G.J., Siemens, J., Geisler, R., Schuster, S.C., Müller, U., Nicolson, T., Tübingen 2000 Screen Consortium. 2004. Mutations in cadherin 23 affect tip links in zebrafish sensory hair cells. *Nature* 428: 955–959. [Medline] [CrossRef]
32. Sotomayor, M., Weihofen, W.A., Gaudet, R., and Corey, D.P. 2012. Structure of a force-conveying cadherin bond essential for inner-ear mechanotransduction. *Nature* 492: 128–132. [Medline] [CrossRef]
33. Steel, K.P. and Bock, G.R. 1983. Hereditary inner-ear abnormalities in animals. Relationships with human abnormalities. *Arch. Otolaryngol.* 109: 22–29. [Medline] [CrossRef]
34. Wada, T., Wakabayashi, Y., Takahashi, S., Ushiki, T., Kikkawa, Y., Yonekawa, H., and Kominami, R. 2001. A point mutation in a cadherin gene, *Cdh23*, causes deafness in a novel mutant, *Waltzer mouse niigata*. *Biochem Biophys Res Commun* 283: 113–117. [Medline] [CrossRef]
35. Wade, C.M., Kulbokas, E.J. 3rd., Kirby, A.W., Zody, M.C., Mullikin, J.C., Lander, E.S., Lindblad-Toh, K., and Daly, M.J. 2002. The mosaic structure of variation in the laboratory mouse genome. *Nature* 420: 574–578. [Medline] [CrossRef]
36. Willott, J.F. 1986. Effects of aging, hearing loss, and anatomical location on thresholds of inferior colliculus neurons in C57BL/6 and CBA mice. *J. Neurophysiol.* 56: 391–408. [Medline]
37. Wilson, S.M., Householder, D.B., Coppola, V., Tessarollo, L., Fritzsch, B., Lee, E.C., Goss, D., Carlson, G.A., Copeland, N.G., and Jenkins, N.A. 2001. Mutations in *Cdh23* cause nonsyndromic hearing loss in waltzer mice. *Genomics* 74: 228–233. [Medline] [CrossRef]
38. Xu, Z., Ricci, A.J., and Heller, S. 2009. Rethinking how hearing happens. *Neuron* 62: 305–307. [Medline] [CrossRef]
39. Yonezawa, S., Yoshizaki, N., Kageyama, T., Takahashi, T., Sano, M., Tokita, Y., Masaki, S., Inaguma, Y., Hanai, A., Sakurai, N., Yoshiki, A., Kusakabe, M., Moriyama, A., and Nakayama, A. 2006. Fates of Cdh23/CDH23 with mutations affecting the cytoplasmic region. *Hum. Mutat.* 27: 88–97. [Medline] [CrossRef]
40. Zheng, Q.Y., Scarborough, J.D., Zheng, Y., Yu, H., Choi, D., and Gillespie, P.G. 2012. Digenic inheritance of deafness caused by 8J allele of myosin-VIIA and mutations in other Usher I genes. *Hum. Mol. Genet.* 21: 2588–2598. [Medline] [CrossRef]
41. Zheng, Q.Y., Yan, D., Ouyang, X.M., Du, L.L., Yu, H., Chang, B., Johnson, K.R., and Liu, X.Z. 2005. Digenic inheritance of deafness caused by mutations in genes encoding cadherin 23 and protocadherin 15 in mice and humans. *Hum. Mol. Genet.* 14: 103–111. [Medline] [CrossRef]